Journal of the Geological Society, London, Vol. **156**, 1999, pp. 435–448. Printed in Great Britain

Palaeoclimate and palaeoenvironmental responses in the western Mediterranean over the last 140 ka: evidence from Mallorca, Spain

JAMES ROSE, XINGMIN MENG & CLARE WATSON

Department of Geography, Royal Holloway, University of London, Egham, Surrey, TW20 0EX, UK

(e-mail: j.rose@rhbnc.ac.uk)

Abstract: Climatic change in the western Mediterranean basin over the last 140 ka has been investigated from sediment and soil sequences along the coast of the northeastern part of Mallorca, Spain. Palaeoclimate and palaeoenvironments are reconstructed from sediment and soil structures, marine and terrestrial molluscan fauna, grain size distributions, mineral magnetics, sediment and soil chemistry, SEM and oxygen isotope values. Dating is by OSL and amino acid geochronometry along with marine molluscan faunal assemblages. All Oxygen Isotope stages and substages from OIS 6 to 1 are recorded. Mean annual temperatures (m.a.t.) of *c.* 19.2°C for the climatic optimum of the Last Interglacial compare with *c.* 17.3°C for the present, and are associated with high sea level, extensive woodland and stable soils, although wide temperature ranges are detected during this stage with values as low as *c.* 10.3°C. Through OIS 5d to 5a m.a.t. fluctuated from 8.2°C to 17.9°C. Low sea level, open vegetation, effective river activity and aeolian sand and dust deposition characterize 5d and 5b while relatively high sea-level and soil development on stable landscapes dominate OIS 5c and 5a. OIS 4 is represented by m.a.t. of *c.* 4.9°C with aeolian sand and loess deposition, limited river activity and weak soil development. Loess deposition persisted into OIS 3, but at this time the m.a.t. was *c.* 13°C and with higher humidity and vegetation growth. During the LGM (OIS 2) m.a.t. was *c.* 8.1°C and effective river, slope and aeolian processes, along with associated with limited vegetation cover, were responsible for the most extensive changes in the landscape. Major rates of change occur during periods of climatic deterioration when the high levels of geomorphic energy were imposed on a landscape undergoing a breakdown of vegetation cover.

Keywords: Mediterranean, palaeoclimates, palaeoenvironment, loess, palaeosols.

The NERC TIGGER IIc project was designed to investigate the change of climate, and the environmental response to these changes in the Mediterranean region over the period from the Last Interglacial (Oxygen Isotope Stage 5e) through the climatic oscillations of the later part of OIS 5 to the globally glacial conditions of OIS 4 and 2. This investigation is of critical importance in providing the only realistic analogue for the changes that would occur within the natural environment should the present 'interglacial' conditions again revert to a 'glacial' mode. Furthermore, this study is designed to provide a sample based on long-term evidence for the way the natural environment of the Mediterranean region will respond to climatic changes, both warming and cooling.

The importance of this study is emphasized by the marked contrast that exists between the 'interglacial' and 'glacial' climates and environments of the Mediterranean region (Tzedakis & Bennett 1995). At the present time Mediterranean regions are located within the boundary zone between the subtropical and mid-latitude atmospheric patterns (Perry 1981; Macklin *et al.* 1995) and are represented by an environment with high sea-levels, dense vegetation cover, relatively high infiltration and moderate river discharges. In contrast, 'glacial' periods are considered to be influenced by the development of a fixed anticyclone over the north European ice sheet and colder sea surface temperatures (Rognon 1987) which produced colder and drier conditions, but increased the seasonality of precipitation (Prentice *et al.* 1992), and are represented by relatively low sea levels, open vegetation with extensive areas of bare ground and loose sediments, soils affected by high physical stresses and highly peaked river regimes. Between these extremes a number of intermediate conditions and environmental responses are likely to have existed, but the process of change, either from warm to cold, or cold to warm is little documented and little understood. This work aims to describe the characteristics of the climate and the physical and biological environment of part of the western Mediterranean region over the last 140 000 years and to discuss the factors that have contributed to the major changes in the landscape. This period encompasses the period from the Last Interglacial through to the Last Glacial Maximum and there are no known effects of human environmental change.

Palaeoenvironments have been interpreted from sediment and soil structures, geomorphological position, grain size distributions, sediment chemistry, and mineral magnetics. Climate has been derived from marine and terrestrial molluscan fauna, SEM analysis and carbon and oxygen isotope signals. Dating is by OSL and Amino Acid geochronometry and biostratigraphy based on marine molluscan assemblages.

Location

The area studied is at Calo d'es Cans and Waterfront Cove in the north east part of the island of Mallorca (Fig. 1) where stacked successions of marine, fluviatile, colluvial, and aeolian deposits are interspersed by soils. The sites are coastal sections located at the base of small river catchments in a position that is sensitive to coastal, river, wind, slope and soil forming processes.

Mallorca is one of the Balearic islands in the western Mediterranean which currently experiences a Mediterranean-

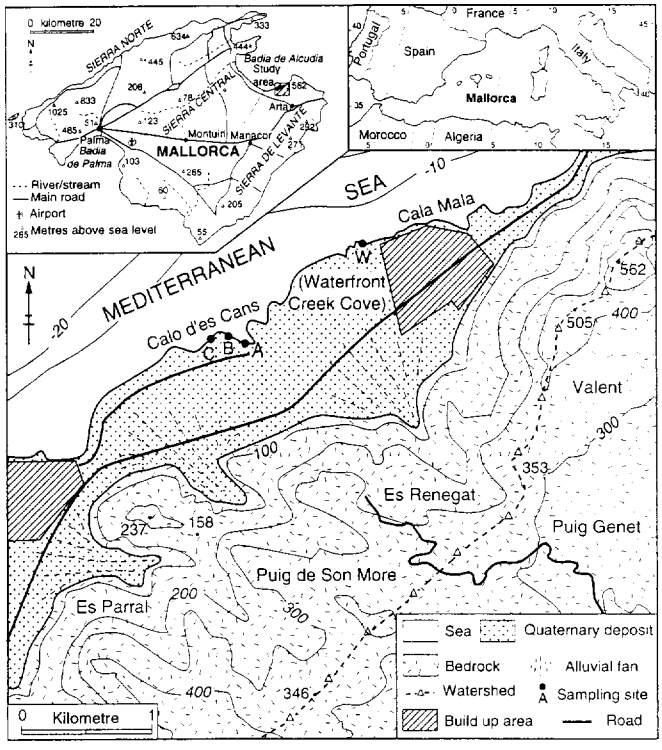

Fig. 1. Location of sampling sites at Calo d'es Cans and Waterfront Cove, northeast Mallorca.

type climate characterized by hot dry summers and mild moist winters. Within this climatic regime the natural geomorphological scenario is coastal activity at a globally high sea level, fluvial processes in ephemeral channels, relatively thick chemically altered soils and relatively stable hillside slopes protected by a dense vegetation cover. All of these conditions are represented at the study area although the last two characteristics have been much changed by human activity. Mean annual temperature in the region is in the order of 17°C with mean January and July values of 10 and 24.5°C respectively. Mean annual precipitation is about 500 mm of which some 90% falls between September and May. The relief in the study region is in the order of 400 m (Fig. 1) and the rock types are predominantly limestones with occasional shales.

Field Description, sampling strategy and laboratory analyses

Four sections were studied in detail (Fig. 2), Calo d'es Cans A, B and C and Waterfront Cove, each of which includes different facets of the lithological and pedological units, but together give a detailed and comprehensive succession (Fig. 3). Each site was precisely levelled with reference to present day mean sea-level (m.s.l.) and the lithofacies were described in the field with respect to sedimentary structure, soil structure, texture, colour, and magnetic susceptibility. Precisely levelled-in samples were collected for laboratory analysis of particle size, additional magnetic susceptibility properties, microfabric, extractable iron, calcium carbonate content (Gale & Hoare 1991), carbon and oxygen stable isotope geochemistry, terrestrial and mollusc amino acid analysis and OSL dating (not all of these results are used in this paper).

Colour determinations are moist Munsell Soil Colors of the sediment or soil matrix. Mottling was recorded where developed. The size of samples used for particle size analysis fulfils the minimum weight defined by British Standards 812 (British Standards Institution 1985). Many of the samples were weakly cemented and disaggregation was achieved by gently crushing with a rubber pestle, followed by immersion with regular stirring in a 0.5% sodium hexmetaphosphate dispersant for 24 hours. Finally the sample and dispersant were placed in an ultrasonic bath for 15 minutes. The size distribution of clasts coarser than 63 μm have been determined by wet sieving and the fraction <63 μm by analysis with a Sedigraph 5100 (Coakley & Syvitski 1991). Results of particle size analysis are shown on Fig. 4 and results of mineral magnetic measurements, free iron measurements and $CaCO_3$ determinations are shown on Fig. 5.

Climatic proxies

Molluscan ecostratigraphy indicated that the lower beach sediments contain a warm water fauna typical of recent interglacials (Butzer & Cuerda 1962; Hillaire-Marcel *et al.* 1996). Marine and terrestrial fauna were also collected from other parts of the succession, but failed to provide reliable climatic information because of limited sample size, limited assemblages and complex taphonomy.

Oxygen isotope signatures from un-abraded marine mollusca taken from the beach deposits and soil cements were used to estimate the temperature of the sea during the life of the selected marine mollusca and the mean annual temperature during carbonate precipitation within the sediments and soils at the study sites. This assumes that the isotope fractionation between calcium carbonate and water is in equilibrium with the environment and the composition of the fluid from which the mineral was precipitated (Marshall 1992; Quade *et al.* 1989, 1994). The process is described in terms of the isotope exchange reaction (O'Neil *et al.* 1969):

$$1/3CaC^{16}O_3 + H_2{}^{18}O <==> 1/3CaC^{18}O_3 + H_2{}^{16}O. \quad (1)$$

Temperature estimates assuming equilibrium fractionation are derived from the equation of O'Neil *et al.* (1969) revised by Hays & Grossman (1991):

$$T(°C) = 16.9 - 4.2(\delta c - \delta w) + 0.13(\delta c - \delta w)^2 \quad (2)$$

where δc is the $\delta^{18}O$ of CO_2 produced by reaction of $CaCO_3$ in phosphoric acid at 25°C and δw is the $\delta^{18}O$ of CO_2 in equilibrium with water at 25°C, both referred to the PDB standard (Epstein *et al.* 1953; Craig 1965) The oxygen isotopic composition of ocean water at Mallorca is 1.10 PDB (Cornu *et al.* 1993) and the meteoric water is −4.5 SMOW (Lecolle 1985) which can be converted to −34.305 PDB by using the conversion equation of Tucker & Wright (1990):

$$\delta^{18}O\ PDB = 0.97006\ \delta^{18}O\ SMOW - 29.94. \quad (3)$$

The reliability of this procedure with regard to marine fauna was tested using recently living molluscs from a site with known present day sea-surface temperatures, and found to provide a reliable estimate of this value.

The isotopic composition of CO_2 was determined using a Prism Series II Isotope Ratio Mass Spectrometer (VG Isotech) according to the reaction:

$$3CaCO_3 + 2H_3PO_4 ===> 3CO_2 + 3H_2O + Ca_3(PO4)_2. \quad (4)$$

All isotopic values are expressed as ‰ PDB standard with a precision of ± 0.03‰. XRD analysis was used to determine the mineralogy and 0.3 mg of calcium was used for each sub-sample.

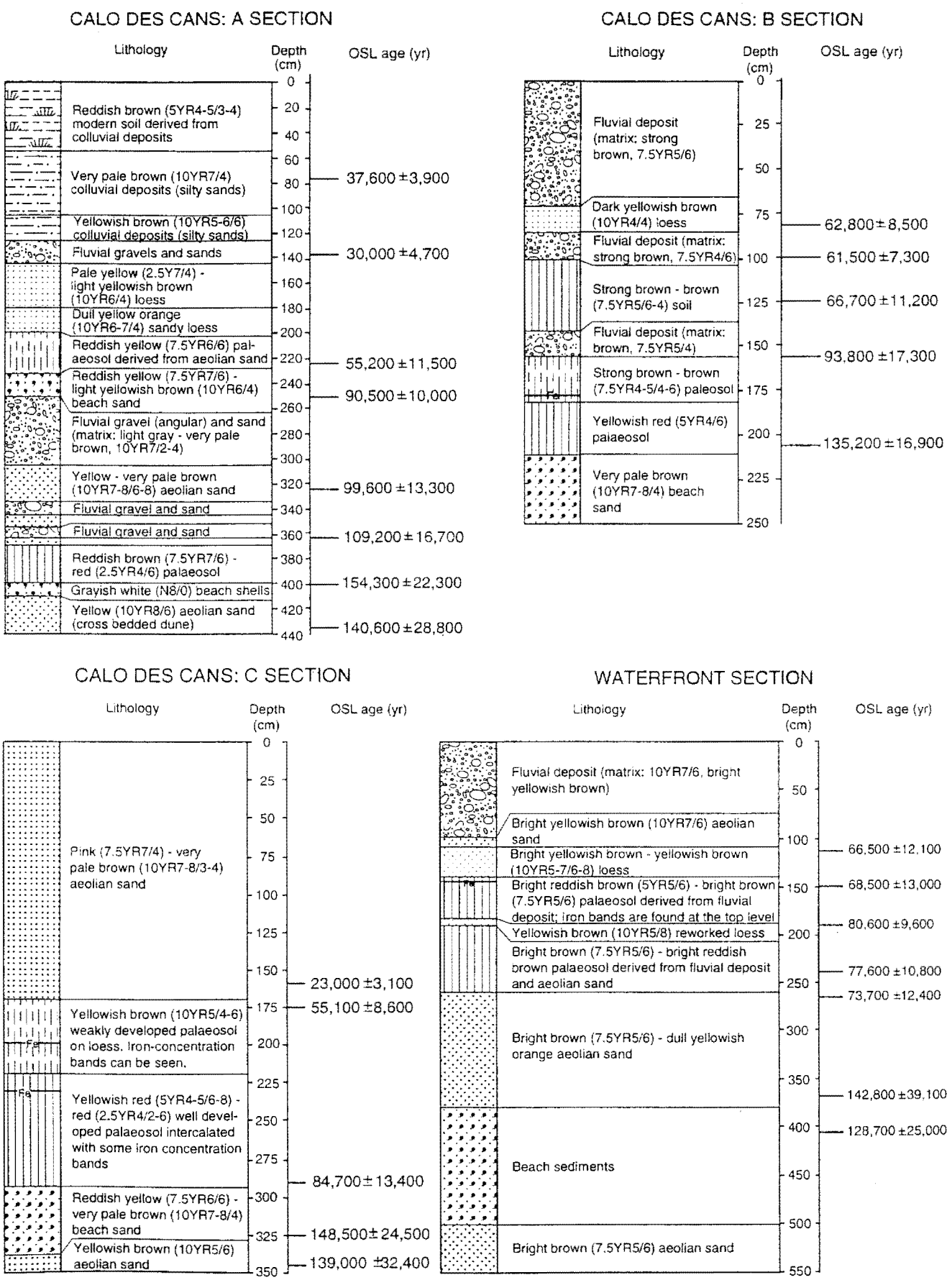

Fig. 2. Sediment and soil logs at the sampling sites at Calo d'es Cans and Waterfront Cove, northeast Mallorca. Each sedimentary and soil unit is described in terms of lithology, colour and depth below the top of the section. The evidence for lithological and pedological interpretations is given in the text and in Figs 4, 5 and 6. OSL ages are also given.

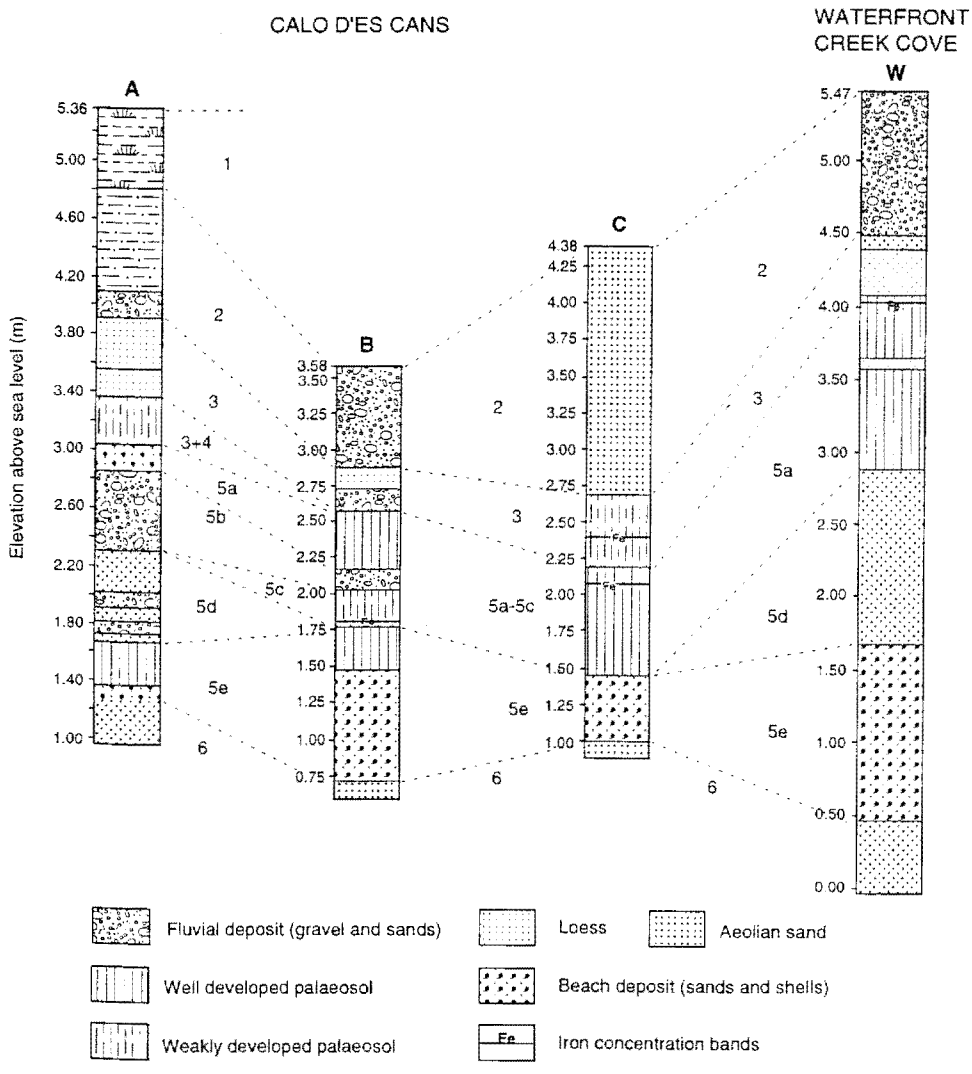

Fig. 3. Correlation of Calo d'es Cans and Waterfront Cove sections, giving elevation above sea level, lithological and pedological interpretation of each unit and Oxygen Isotope Stages.

Material for isotopic study was examined under the microscope, and the carbonate cement and molluscs were abstracted with a fine pin or brush. Samples of cement were selected only from the skeleton-grain coatings, and carbonate associated with nodules and leaching tubes which represent prolonged, and later stages of soil activity, were avoided.

A total of 95 samples were studied from soil cements, all of which were replicated, or run three times if there was significant variance, and each sample point is represented by a mean value. Eight samples were studied from marine molluscs collected from beach sediments and each sample is represented by a mean value based on two or three analyses. Wherever possible samples were taken for stable isotope analysis at 10 cm intervals through each of the sections (44 from section A, 15 from section B, 22 from section C and 22 from W section). Results of these studies are given in Table 1.

Initially, an attempt was made to estimate precipitation using magnetic susceptibility, following the studies of Maher & Thompson (1992, 1995) in western China, but investigations carried out in Mallorca during this study indicated that these assumptions are not applicable in Mediterranean regions and that decomposed plant litter was a major source of the magnetic signal, rather than the precipitation-determined climatic processes (Meng *et al.* 1997). As a result, it was decided to use the SEM image of soil cement to give a qualitative estimate of the climate in existence during soil formation. An open cement lattice is considered indicative of arid conditions, well developed bridge lattices are considered indicative of moderate precipitation and dense cement matrix is considered to represent humid conditions. Representative images are given in Fig. 6 and the interpretations are summarized in Table 1.

Dating methodology

A molluscan fauna typical of the lower beach unit has been dated elsewhere in Mallorca by U-Series measurements to between *c.* 135 ka and *c.* 117 ka BP (Hillaire-Marcel *et al.* 1996), confirming the Last Interglacial age of this unit.

Because of the extensive use of aminostratigraphy within the Mediterranean, and especially Mallorca (Hearty *et al.* 1986; Hearty 1987) this technique was applied to 20 samples of the gastropod (*Bittium* sp.) from sections Calo d'es Cans A and B. D-alloisoleucine to L-isolucene ratios (alle:Ile) have been determined on the total amino-acid fraction using an automated ion-exchange HPLC amino acid analyser as described by Sykes (1991).

As elsewhere, these results have insufficient precision to date the individual lithostratigraphic units, but the groups of ratios do identify two separate events which resulted in the deposition of beach sediment at the locality, and they also show that this beach sand was subsequently extensively reworked by aeolian processes (Fig. 7). The Last Interglacial beach is represented by five determinations which give a

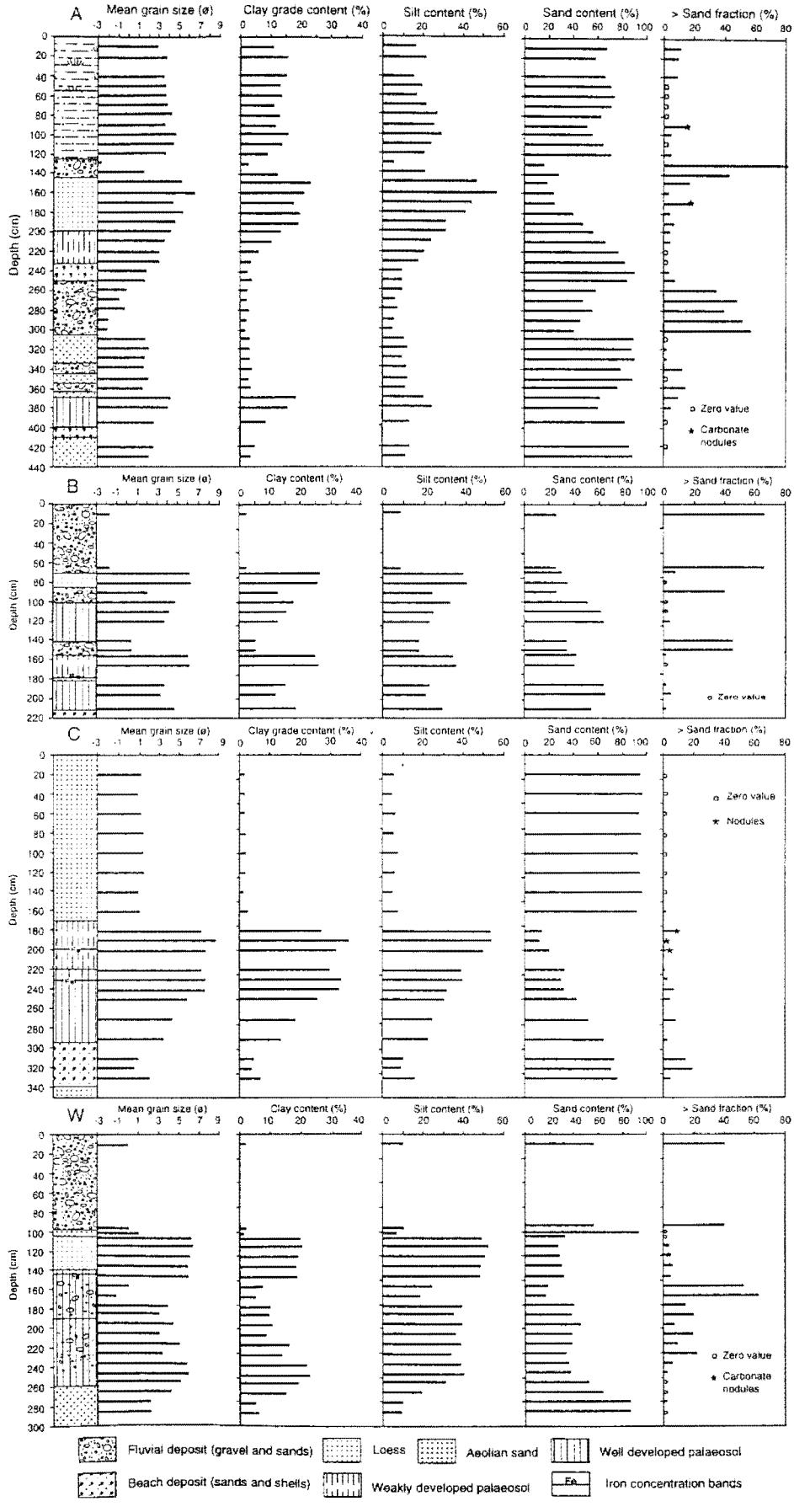

Fig. 4. Particle size properties of sediments in the sections from Calo d'es Cans and Waterfront Cove. Size distributions are given in terms of phi mean, % clay (<2 μm), % silt (2–64 μm), sand (64 μm–2 mm) and gravel (>2 mm) fractions. An asterisk is used to indicate where soil nodules constitute the gravel fraction. $\delta^{18}O$ value is given in terms of ‰ PDB.

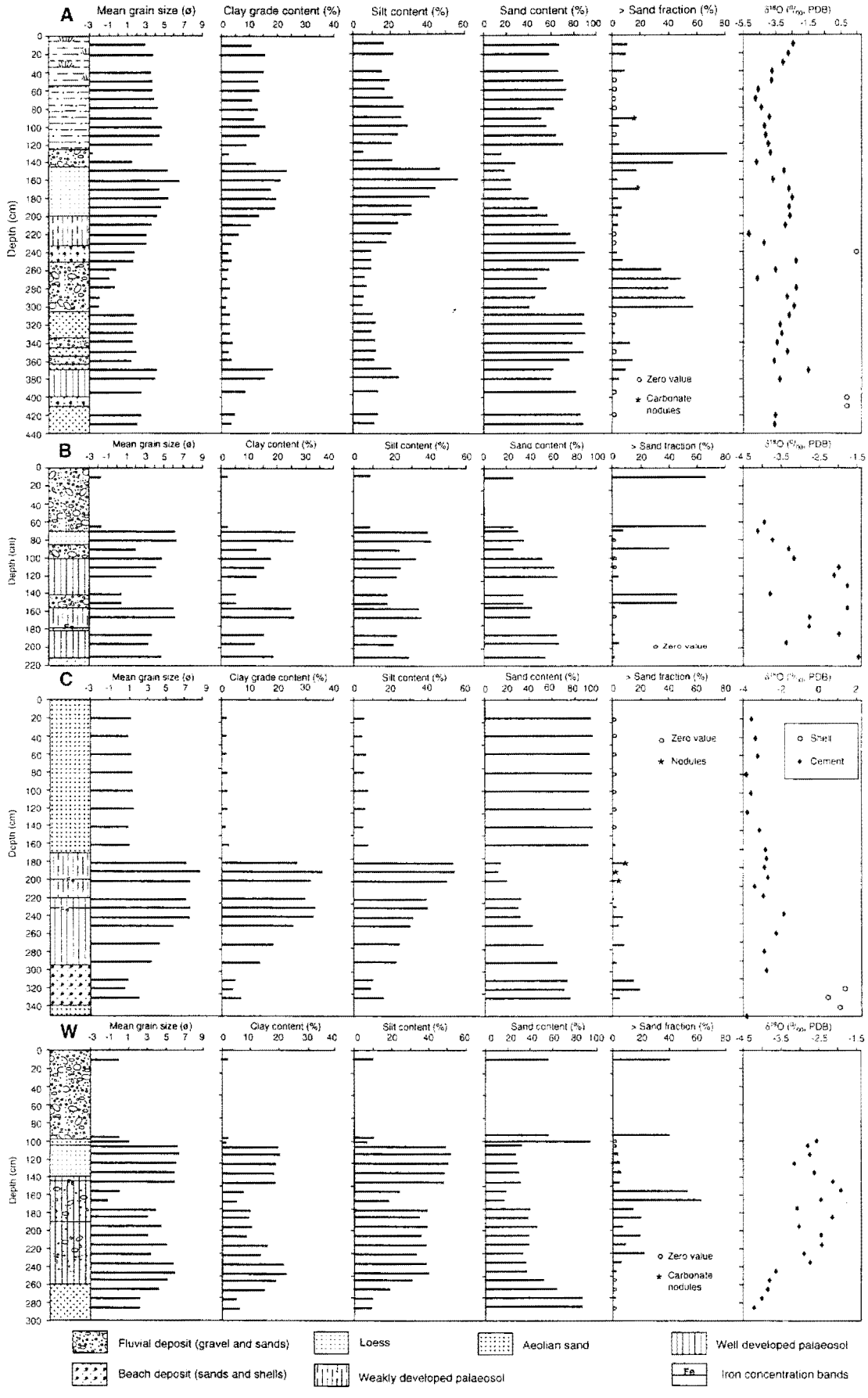

Fig. 5. Mineral magnetic properties, and extractable iron and calcium carbonate contents of sediments and soils in the sections from Calo d'es Cans and Waterfront Cove. Mineral magnetics is given in terms of susceptibility (MS SI units) absolute difference between high and low frequency susceptibility values (χ^{l-h}). Extractable iron is given total iron (Fet), AAO extractable iron (Feo) and CBD extractable iron (Fed) in parts per million. Calcium carbonate values relate to the percentage within the fraction <63 μm. ◇ values are derived from soil cement and ○ are derived from marine molluscs.

Table 1. *Summary of results and climatic and environmental interpretations from Cala d'es Cans and Waterfront Cove, northeast Mallorca*

Landform, sedimentary and soil properties	Biological evidence	OSL ages (ka)	MAT (°C)	Moisture regime	Environment	OIS
Sandy loam with increasing upwards clay, humus, MS and Fe values	Terrestrial mollusc fauna			Moist	Slopewash transporting soil materials from adjacent hillside slopes	1
Thick beds of sands and gravels and well-sorted, cross-bedded sand	Derived marine molluscan fragments and terrestrial mollusc fauna	30–23 ± 5–3	13.4–6.3	Very dry	Fluvial deposition of large alluvial fans and extensive aeolian dunes beyond influence of the rivers	2
Yellowish brown silt, with weak soil development at surface. Far-travelled mineral composition. Low MS, moderate Fe value	Terrestrial mollusc fauna	67–55 ± 11.5–7	14.6–9.9	Moist	Loess deposition from distant sources	3
Gravels with brown sandy matrix, and sands with increasing-upwards clay content, moderate MS and Fe value	Derived fragmented molluscs	61–55 ± 12–8	8.2–4.9		Fluvial gravels and aeolian sand, weathered at surface	4
Reddish yellow, well-sorted medium and coarse sand. Brown soil with high MS, Fe and clay values	Marine molluscan fauna	90–73 ± 17–10	17.9–10.3		Coastal deposition of beach ridge	5a
Sub-angular gravel and sands. Low MS and Fe value		94 ± 17	10.8–6.7		Fluvial deposition of material eroded from adjacent hillsides	5b
Brown, clayey soil on silty parent material. Moderate MS and high Fe value. Local Fe pan			17.9–13.6		Loess with temperate soil formation	5c
Well-sorted sands and bimodal sands and gravels. Low MS and Fe value except at base	Derived fragmented mollusca	109 ± 17	13.6–8.2		Aeolian sand and fluvial sands and gravels	5d
Red, clayey soil, with high MS, and Fe values and chemically fretted $CaCO_3$ fragments		135 ± 17	19.5–11.3	Moist	Mediterranean type soil formation	5e
Pale brown medium and coarse sand	Marine molluscan fauna	154–129 ± 25–22	19.5–17.9	Moist	Coastal deposition of ridges and beaches	5e
Erosional platform					Shoreline erosion	
Bright brown, well sorted, cross-bedded sand		140 ± 30	10.2	Very dry	Aeolian deposition of dunes	6

MS, magnetic susceptibility; MAT, mean annual temperature; OIS, oxygen isotope stage.

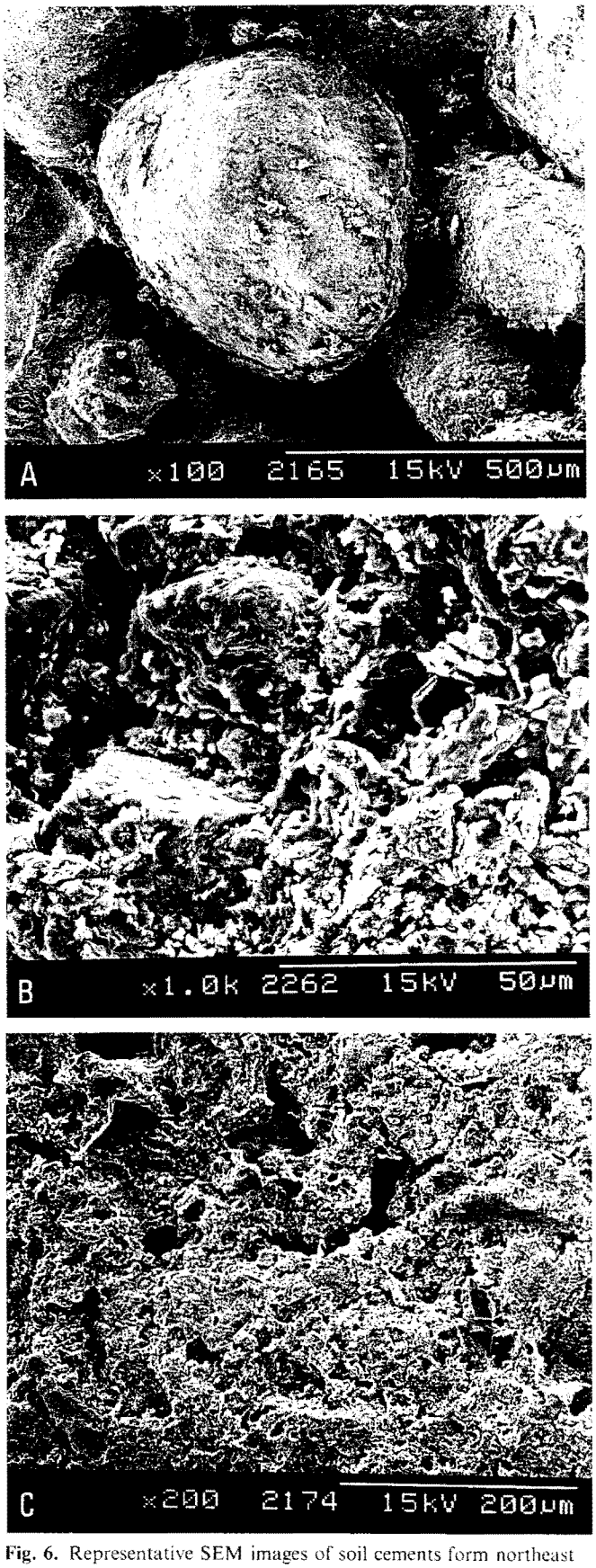

Fig. 6. Representative SEM images of soil cements form northeast Mallorca. A is an open cement lattice indicative of arid conditions, B is a well developed bridge lattices structure indicative of moderate precipitation and C is a dense cement matrix representative of soil formation in humid conditions.

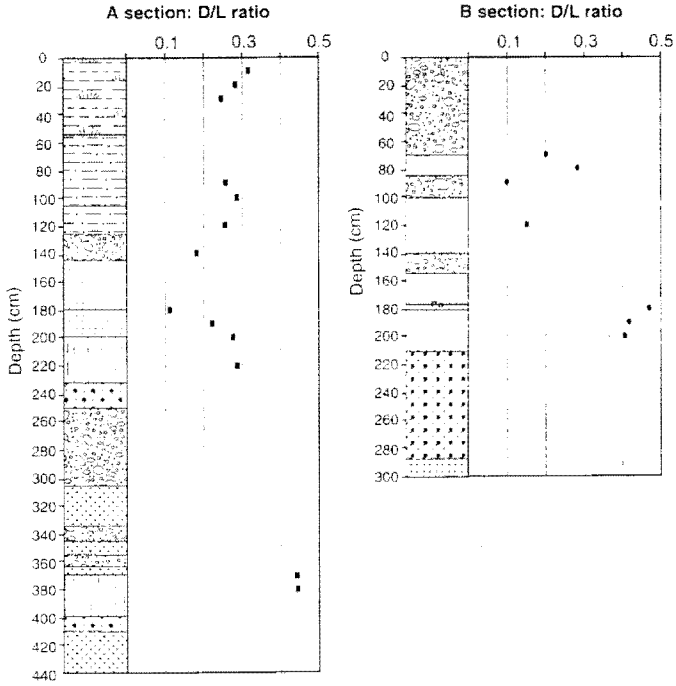

Fig. 7. Individual amino acid racemisation ratios on *Bittium* sp. taken from Calo d'es Cans sites A and B. The determinations separate the upper beach unit (OIS 5a) from the lower beach unit (OIS 5e). The *Bittium* shells in the upper beach have been substantially reworked by wind to constitute a significant proportion of the material in the upper aeolian dunes.

mean *D/L* ratio of 0.434 ± 0.024. A quite separate, later event is indicated by the introduction of a new fauna, with a *D/L* ratios of between 0.31 and 0.11 ($n=15$, mean $=0.229 \pm 0.067$), and is related to the high sea-level widely recognized in the western Mediterranean associated with OIS 5a (Zazo *et al.* 1998).

Optically stimulated luminescence (OSL) is the main method that has been used to date the sequences (Aitken 1985). 25 measurements have been made on quartz grains in the 180–125 µm size range from beach sand, aeolian sand, loess, fluvial sand and soil materials, and the results are represented in Table 1 and the details of the appropriate measurements are given in Table 2. Blocks of sediment with the dimension $20 \times 20 \times 20$ cm were collected from the sections, wrapped in light-proof black polythene bags, and transported back to the laboratory. All samples were prepared and analysed following the procedures of Rhodes (1988). The outer parts of the sample block were scraped-off in the laboratory under conditions of subdued orange light, and the inner part was crushed and treated with 38% HCl to remove the $CaCO_3$. Samples were then washed using distilled water, dried at *c.* 50°C and sieved to extract the 180–125 µm fraction. This was then treated with 40% HF and stirred for 60 minutes to remove feldspars, clay minerals and the outer 10 µm of the quartz grains. After washing with dilute HCl, acetone and distilled water, the quartz was separated from the heavy mineral fraction using a sodium polytungstate solution with a density of 2.67. Finally, the sample was further washed, dried and sieved to collect the fraction >125 µm. The samples were mounted on 1 cm diameter aluminium discs using silicone oil and measurements of OSL were made using an automated Riso set with a filtered halogen light source.

The results of the OSL determinations are listed in Table 2 and shown on Fig. 3 in relation to the lithology sampled. Errors range from 20 to 10%, but the ages display consistent trends adding considerably to their reliability and significance. Using this method, in conjunction with the biostratigraphy and aminostratigraphy of the beach sediments, it is possible to derive a chronology for the stratigraphic and soil units formed between OIS 6 and OIS 2, bearing in mind the errors on the determinations and stratigraphic correlations between sites.

Table 2. *OSL age estimates from quartz grains in the 180–125 μm size range from beach sand, aeolian sand, loess, fluvial sand and soil materials. Calo d'es Cans and Waterfront Cove, northeast Mallorca*

Section and sample	K% of sed. grain	Assumed external α-dose rate (μGy a^{-1})	External β-dose rate (μGy a^{-1})	External γ+cos. dose rate (μGy a^{-1})	Cosmic dose rate (μGy a^{-1})	Total dose rate (μGy a^{-1})	DE (Gy)	Age (ka)	Infered $\delta^{18}O$ stage
A-70	0.41 ± 0.02	1 ± 1	495 ± 25	527 ± 23	158.42 ± 15.80	1023 ± 44	38.48 ± 3.59	37.6 ± 3.9	2
A-130	0.55 ± 0.03	1 ± 1	580 ± 32	532 ± 23	142.97 ± 14.29	1113 ± 51	33.39 ± 5.00	30.0 ± 4.7	2
A-220	0.42 ± 0.02	1 ± 1	490 ± 26	470 ± 20	122.57 ± 12.30	961 ± 43	53.09 ± 10.83	55.2 ± 11.5	4
A-250	0.12 ± 0.01	0 ± 0	193 ± 10	268 ± 14	116.43 ± 11.6	461 ± 21	41.73 ± 4.13	90.5 ± 9.9	5a
A-320	0.15 ± 0.01	0 ± 0	260 ± 15	304 ± 14	103.29 ± 10.30	564 ± 27	56.20 ± 7.01	99.6 ± 13.3	5d
A-360	0.11 ± 0.00	0 ± 0	234 ± 13	295 ± 14	96.46 ± 9.65	529 ± 24	57.79 ± 8.44	109.2 ± 16.7	5d
A-390	0.10 ± 0.00	0 ± 0	280 ± 15	324 ± 15	90.85 ± 9.08	605 ± 28	93.31 ± 12.79	154.3 ± 22.3	5e
A-430	0.10 ± 0.00	0 ± 0	279 ± 16	318 ± 15	85.57 ± 8.56	597 ± 29	83.90 ± 16.69	140.8 ± 28.8	6
C-160	1.18 ± 0.06	2 ± 2	1070 ± 64	805 ± 35	135.82 ± 13.5	1877 ± 94	43.14 ± 5.49	23.0 ± 3.1	2
C-170	1.18 ± 0.06	2 ± 2	1063 ± 63	803 ± 35	133.5 ± 13.4	1868 ± 93	102.95 ± 15.16	55.1 ± 8.6	3
C-290	0.50 ± 0.03	1 ± 1	610 ± 35	556 ± 23	108.73 ± 10.8	1168 ± 55	98.92 ± 14.9	84.7 ± 13.4	5c
C-320	0.10 ± 0.00	0 ± 0	235 ± 13	295 ± 14	103.29 ± 10.3	530 ± 24	78.75 ± 12.49	148.5 ± 24.5	5c
C-340	0.04 ± 0.00	0 ± 0	170 ± 10	252 ± 13	99.82 ± 9.9	422 ± 20	58.70 ± 13.40	139.0 ± 32.4	6
B-80	0.85 ± 0.04	2 ± 2	929 ± 51	808 ± 34	155.74 ± 15.50	1736 ± 79	109.06 ± 13.9	62.8 ± 8.5	3
B-100	0.64 ± 0.03	1 ± 1	689 ± 38	634 ± 27	150.50 ± 15.05	1324 ± 60	81.44 ± 9.04	61.5 ± 7.3	3
B-120	0.54 ± 0.03	1 ± 1	583 ± 32	553 ± 24	145.44 ± 14.50	1137 ± 51	75.89 ± 12.23	66.7 ± 11.2	5a
B-155	0.98 ± 0.05	2 ± 2	1019 ± 57	850 ± 36	136.98 ± 13.70	1870 ± 88	175.45 ± 31.31	93.8 ± 17.3	5b
B195	0.35 ± 0.02	1 ± 1	438 ± 24	455 ± 20	127.92 ± 12.79	894 ± 40	120.89 ± 14.07	135.2 ± 16.9	5e
W-115	1.06 ± 0.05	2 ± 2	1139 ± 63	940 ± 39	146.68 ± 14.67	2080 ± 97	138.42 ± 24.35	66.5 ± 12.1	3
W-145	0.68 ± 0.03	2 ± 2	869 ± 47	774 ± 32	139.35 ± 13.9	1645 ± 75	112.68 ± 20.84	68.5 ± 13.0	5a
W-185	0.34 ± 0.02	1 ± 1	533 ± 29	543 ± 23	130.13 ± 13.0	1077 ± 48	86.93 ± 9.65	80.6 ± 9.6	5c
W-235	0.75 ± 0.04	1 ± 1	840 ± 6	701 ± 29	119.46 ± 11.9	1543 ± 71	119.75 ± 15.76	77.6 ± 10.8	5c
W-265	0.45 ± 0.02	1 ± 1	581 ± 31	531 ± 22	113.48 ± 11.3	1113 ± 51	82.05 ± 13.24	73.7 ± 12.4	5d
W-360	0.10 ± 0.00	0 ± 0	193 ± 11	247 ± 12	96.46 ± 9.6	441 ± 20	62.90 ± 16.99	142.8 ± 39.1	5d
W-400	0.13 ± 0.01	0 ± 0	239 ± 14	276 ± 13	90.08 ± 9.00	515 ± 23	66.23 ± 12.59	128.7 ± 25.1	5e

OI Stage is estimated from OSL age and stratigraphic relationships.

Litho- and soil stratigraphy with reconstructed climate

Basal aeolian sand (OIS 6)

This is a bright brown (7.5YR5/6) lithified, cross bedded, well sorted medium sand (Fig. 4) composed primarily of rounded mollusc fragments, and found at the base of each of the sections (Fig. 2). Two OSL determinations gave ages of around 140 ka ± 30 (Fig. 2). The sedimentary structures, degree of sorting, composition and texture of grains suggest aeolian transport and sorting of sea-bed or beach sand representing an extensive dune-field in the study area. Temperature at this time was in the order of 10.2°C, the moisture regime was very dry and biomass was limited.

Lower beach sand and soil (OIS 5e)

This is a very pale brown (10YR7-8/4) medium and coarse sand (Fig. 4) with abundant whole and fragmented molluscs, and is represented at all the sections (Figs 2 and 3). The size distribution and the fauna indicate a beach sediment while the variations in size range and degree of shell fragmentation indicate variable shoreline energy at the different sites, probably due to different positions on the palaeo-coastline. Four OSL determinations give ages in the range 154–128 ± 25–16 ka (Fig. 2). The range of ages, the amino acid ratios and the molluscan fauna suggest that this unit was formed during the optimum of the Last Interglacial (OIS 5e). Temperature at this time was in the order of 19.5–17.9°C, the moisture regime was moist with extensive biomass cover.

Strongly developed soil properties are superimposed on the upper part of the Lower Beach Sand at all the Calo d'es Cans sites, although they are absent at Waterfront Cove where the top of the beach is eroded. This soil is a reddish brown (7.5YR7/6) to yellowish red (5YR4/6) and red (2.5YR4/6) colour with between 10 and 40% clay, contrasting with maximum values of about 7% clay in the beach parent material (Fig. 4). High iron and magnetic susceptibility values characterize this unit and $CaCO_3$ content is much diminished relative to the beach sand (Fig. 5). Temperature at this time was in the order of 19.5–11.3°C, and the moisture regime was moist with extensive biomass cover.

Lower aeolian sands, fluvial gravels and loess with soil imprints (OIS 5d-a)

This is a lithostratigraphic complex with up to four separate sediment/soil units. The most complete succession is at Calo d'es Cans B where all but the lowest unit is represented (Figs 2 and 3). At Calo d'es Cans C the whole succession is represented by a very strongly developed soil. Calo d'es Cans A, which is closer to a valley axis is dominated by fluviatile sediments, and this site and Waterfront Cove also include thin beds of aeolian sand.

The lowest unit of this complex is interbedded aeolian sand and fluvial gravels, represented at Calo d'es Cans A. The genesis of these units is indicated by their structure and size distribution (Fig. 4). High magnetic mineral content of the basal sands and gravels suggests incorporation of soil material

(Fig. 5) from the underlying beach. The rapid changes of lithology reflect the relative influence of river and wind transport and deposition, almost certainly influenced by the geomorphological position of the locality. OSL ages of 109–99 ± 13–10 ka (Fig. 2) on the sand units indicate that these deposits were likely to have been formed in OIS 5d. At Waterfront Cove well-sorted aeolian sands are the equivalent unit. Temperature at this time was in the order of 13.6–8.2°C, the moisture regime was dry and biomass was low.

The next unit in this complex is a strong brown/brown (7.5YR4-5/4-6) soil, developed on a silt-rich parent material, probably loess (Fig. 4). Clay and extractable iron content is high although magnetic susceptibility values are moderate (Fig. 5). Locally an iron pan is developed. All these properties reflect soil formation, but with a parent material that readily yields clay size material and iron minerals, relative to the lower soil developed on the beach sands. The age of this unit cannot be determined directly but it is likely to be OIS 5c. Temperature at this time was in the order of 17.9–13.6°C, the moisture regime was moist and biomass was relatively low.

Overlying this brown soil at Calo d'es Cans A and B is a sub-angular gravel with brown (7.5YR5/4) sand, typical of the coarse grained fluviatile sediments derived from the local bedrock in the area. Low mineral magnetic and extractable iron values indicate composition (Fig. 5) of material derived from freshly eroded limestones and an OSL determination on a sand bed gives an age of around 94 ± 17 ka suggesting formation during OIS 5b (Fig. 2). Temperature at this time was in the order of 10.8–6.7°C. Information is not available to determine the moisture regime but the biomass cover is estimated as moderate.

The final unit of this complex is a reddish yellow (7.5YR7/6) and light yellowish brown (10YR7/2-4) beach sand at Calo d'es Cans A and a soil at all the other sites. The genesis of this beach sand is indicated by the size distribution (Fig. 4) and newly introduced molluscan fauna. Amino acid ratios from the molluscan fauna in this unit are significantly lower than those in the lower beach unit (Fig. 7), indicating a distinct shoreline event rather than simple reworking of existing coastal and sea-bed materials. The soil, which is in the equivalent stratigraphic position at the other sites, varies in colour depending upon the character of the soil unit and the parent material (Fig. 5). At Calo d'es Cans B, where the soil is developed on fluvial sands and gravels formed in OIS 5b, it is a strong brown (7.5YR5/4-6) colour with moderate magnetic susceptibility values and extractable iron content. At Waterfront Cove, where it is developed on aeolian sand, it is bright brown (7.5YR5/6) to bright reddish brown (5YR5/6) with relatively high magnetic susceptibility and extractable iron values. However at Calo d'es Cans C, where the soil developed on a land surface that came into existence with the fall of sea-level in OIS 5e, the soil horizon is 70 cm thick and the colour is a yellowish red (5YR4-5/6-8) or red (2.5YR4.2-6) with extremely high magnetic susceptibility and extractable iron values and high clay content. This differences in the development of the soil reflect the different lengths of time over which they have formed, so that B section was at the surface for about 10 ka, Waterfront section was at the surface for some 30 ka and C section had been exposed to soil forming processes for some 40 ka, including the latter part of the Last Interglacial (OIS 5e). Temperature at this time was in the order of 17.9–10.3°C, the moisture regime was moist and the biomass cover was high.

Fluvial gravels and aeolian sand altered by soil formation (OIS 4-3)

Fluvial gravels exist at Calo d'es Cans B and aeolian sands are developed at Calo d'es Cans A. These sands are probably derived from sea-bed materials, that have been altered to a reddish yellow (7.5YR6/6) colour, with an increasing-upwards clay content, moderate magnetic susceptibility and moderate extractable iron values (Figs 4 and 5). OSL determinations on this unit give age of around 61–55 ± 11.5–7 ka (Fig. 2), suggesting that the sand was most probably deposited during OIS 4 and that soil formation took place in OIS 3. Temperature at this time was in the order of 8.2–4.9°C, the moisture regime was dry and biomass cover was very low.

Loess (OIS 4)

The next unit in the succession is a silt which is found at all the sites, although at Calo d'es Cans C it is modified by weak soil development. Universally, the silt is a yellowish brown colour, but it varies slightly from a pale yellow (2.5Y7/4) and light to dull yellowish brown (10YR6-7/4) at Calo d'es Cans A to dark yellowish brown (10YR4/4) at B and bright yellowish brown (10YR7/6) at Waterfront Cove. In all cases silt is the dominant size, although there are small amounts of sand and clay (Fig. 4). Mineralogically it is dominated by silica and calcite with minor amounts of feldspars, clays, magnesium minerals and micas and is much more variable than other lithologies in the area. Magnetic susceptibility is low, and extractable iron content is moderate (Fig. 5). All these properties lead to the suggestion that this is a loess, derived from an extensive region rather than local provenance. The common occurrence at all the sites suggests that it occurred universally as rain-out from a dust-charged atmosphere. OSL determinations suggest that it was formed around 67–55 ± 12–8 ka indicating that these conditions occurred during OIS 4 through into OIS 3 (Fig. 2). Temperature at this time was in the order of 14.6–9.9°C, the moisture regime was moist with moderate biomass cover, probably taking the form of grasses.

Fluviatile sands and gravels and aeolian sand (OIS 3-2)

The sands and gravels are at Calo d'es Cans A, B and Waterfront Cove, and the aeolian sand is at Calo d'es Cans C. At all sites these sediments form the thickest sand and gravel unit in the succession. A bimodal size distribution with modes in the −3 and +2 phi ranges (Fig. 4), the sub-angular and sub-rounded form of the clasts, and the poorly developed, low angle sedimentary structures suggest that the sands and gravels were formed by rivers close to the axis of the small valleys that drain down from the local hills. At Calo d'es Cans A and B these gravels are located at the mouth of a shallow valley, but at Waterfront Cove they are part of a fan beyond the valley mouth. Calo d'es Cans C is beyond the influence of these rivers and this site is dominated by large scale cross bedded, very well sorted sands (Fig. 4) composed predominantly of shell and limestone fragments. Magnetic susceptibility (MS) values are very low and extractable iron is absent (Fig. 5). In all respects, the characteristics of this unit indicate aeolian deposition of sand size material as large dunes. The material of which these dunes is composed is derived locally from the adjacent dry sea-bed and seasonally dry braid-plains. OSL ages of the river and dune deposits give ages of 30–23 ± 5–3 ka (Fig. 2) suggesting that deposition took place in the latter part of OIS 3 and

Table 3. *Patterns of environmental change, northeast Mallorca over the last 140 000 years*

OIS	Environment	Climate and operating surface processes
2	Fluvial deposition of large alluvial fans and extensive aeolian sand dune formation beyond the rivers	Period of most significant landscape change with extensive fluvial erosion, transport and deposition, and extensive aeolian dune formation, under cold, arid conditions. Effectiveness of rivers is a consequence of rapid run-off from landscape with low vegetation cover.
3	Loess deposition	High atmospheric dust conditions, but relatively moist, cool climate and sparse vegetation cover, dense enough to trap dust and initiate soil formation.
4	Fluvial gravels and aeolian sand, weakly developed soil at surface	Period with most extreme cold recorded. Initiated by significant landscape change with river and aeolian activity. Replaced by more stable conditions with cool temperate soil development.
5a	Coastal deposition of beach ridge. Temperate soil formation beyond coastline	High sea level, possibly associated with Mediterranean-wide tsunami. Cool temperate, moist climate with landscape stability.
5b	Fluvial deposition of material eroded from adjacent hillsides	Deterioration of climate and breakdown of vegetation. High runoff and fluvial erosion, transport and deposition.
5c	Loess with temperate soil formation	Moist, cool temperate with high atmospheric dust content and loess deposition. Open vegetation trapping silts with weak, temperate, soil formation.
5d	Aeolian sand and fluvial sands and gravels	Climatic deterioration. Vegetation breakdown, effective fluvial erosion, transport and deposition and aeolian transport and deposition of sand sheet, possibly associated with available sea bed sedimants.
5e	Mediterranean type soil formation	Eustatic fall of sea level associated with short-duration climatic deterioration. Mediterranean type climate at other times. No evidence of additional high sea level. Stable landscape with dense vegetation cover and strong chemical weathering in seasonally moist climate.
5e	Coastal deposition of ridges and beaches	Coastal deposition with beach ridges across low relief and beaches fronting cliff lines. Mediterranean-type climate.
5e	Shoreline erosion	Coastal erosion associated with eustatic rise of sea level.
6	Aeolian deposition of dunes	Extensive deposition of unlithified and unvegetated sea bed and coastal sands across arid, sparsely vegetated, land surface.

during OIS 2 which is the Last Glacial Maximum (LGM). Temperature at this time was in the order of 13.4–6.3°C, the moisture regime was very dry but seasonal and biomass cover was moderate becoming very low.

Colluvial sandy loam and humic sandy loam

These deposits are located only at Calo d'es Cans A. These are sandy loams with a high terrestrial mollusc fauna (Fig. 4). The humic content increases upwards through the unit, as does the magnetic susceptibility values and the iron content (Fig. 5). $CaCO_3$ responds inversely with these properties. The size distribution and mollusc fauna suggest that these units formed by mass movement of sandy soil material down hillside slopes. The lowest part of the unit appears to have been formed when soil development was minimal, but the upper part appears to include a high component of soil products. It is suggested that these colluvial units were produced primarily by slope-wash, but that the earlier phase involved only unweathered sandy sediments, whereas the later phase involved a high component of weathered material, probably reflecting soil degradation associated with grazing and agricultural practices.

Discussion

The evidence presented above provides a basis for interpreting the development of the landscape from OIS 6 through to OIS 2 and represents a series of changes of climate that vary from seasonally moist, mediterranean-type climates slightly warmer than now, to relatively cold, arid climates with mean annual temperatures in the order of 5°C. The patterns of change fall within the framework described from south and eastern France by Guiot *et al.* (1989), Reille & de Beaulieu (1990) and de Beaulieu & Reille (1992), by Pons & Reille (1988) in southern Spain, and by Watts *et al.* (1996) in southern Italy . A wide range of geomorphological conditions are associated with these changes of climate and have contributed to distinct patterns of landscape change. The main attributes of the environmental conditions along with the factors responsible for the changes are set out in Table 3.

Warmer climatic episodes

The periods of warmer climate (OIS 5e, 5c, 5a and 3) are characterized by soil development, minimal river activity and landscape stability except for shoreline activity associated with high sea levels. Beach sediments were deposited in OIS 5e and 5a hosting marine molluscan faunas, which were subsequently re-worked during the colder episodes. It is noticeable that the beach sediments formed during OIS 5a do not equate with a period when global sea level was equivalent to levels in existence now or during OIS 5e (Shackleton 1987), but appears to have been deposited by a tsunami event of this age

recognized elsewhere throughout the Mediterranean region (Wood 1997). Soil types vary from red clay- and iron-rich soils with high MS values, formed in the Last Interglacial (OIS 5e), to brown soils with relatively high clay, iron and MS values formed in the less warm periods (OIS 5c, 5a and 3) (Yaalon 1997). Intensity of soil development is not just a function of climate, but also length of time over which the soil has developed at the land surface as can be seen by the much higher clay, iron and MS values that characterize the soil that developed through OIS 5e-a in Calo d'es Cans C relative to the soils that developed through OIS 5e-c in Calo d'es Cans B, and through only the latter part of 5e in Calo d'es Cans A. Soils developed in OIS 5c and 3 are also influenced by loess deposition.

The results from OIS 5e show a complex story that suggests that the Last Interglacial had a variable climate as suggested by Field *et al.* (1994), and GRIP Members (1993) rather than a simple cycle reconstructed by palynological studies of this interglacial (West 1980). Stable oxygen isotopic values indicate that maximum warmth existed during the period of high sea-level conditions at an earlier part of the interglacial, but that after sea level had fallen and a soil began to develop on the beach, temperatures fluctuated between 19.5 and 11.3°C before the temperature fell into the cooler period of OIS 5d.

The explanation for the lack of river activity in these warmer episodes may be found in the effects of vegetation and soil cover in increasing interception and infiltration and reducing runoff (Fuller *et al.* 1998), despite the higher moisture levels indicated by the SEM of the soils and sediments. In the absence of any fluvial sediments from these periods, or even erosion of the soils, it is likely that these small catchments acted as dry valleys throughout these periods and that channel flow was maintained, and hence erosion and deposition took place only in larger catchments than those studied here.

Colder climatic episodes

All the significant landscape changes in the area, except those caused by shoreline activity, took place in the colder episodes. River processes are recognized by deposition of sands and gravels during OIS 5d, 5b, 4 and 3-2 with the most effective river activity recorded during the Last Glacial Maximum (OIS 2) (Rose & Meng 1999). The palaeoclimate estimates for these periods indicate that frost action would have occurred during winter months and that this process would have provided a method of disaggregating soil material over the catchment and facilitating the production of limestone clasts from the well-jointed bedrock outcrops.

At the localities concerned, the river activity consists of the deposition of small alluvial fans over the coastal plain. These river deposits include material with relatively high iron and MS values indicating erosion and deposition of soil material from the hillside slope (base of OIS 5d and OIS 4), and materials with very low iron and MS values indicating erosion of bedrock, suggesting incision in the upper parts of the catchment and erosion of bare hillside slopes (OIS 5b and OIS 2). The river sediments also include derived marine fauna indicating reworking of the earlier beach deposits. The reasons for this river activity, despite the much lower moisture levels at these times is considered to be due to rapid runoff across unvegetated surfaces with thin soils or bare rock surfaces, as recognized elsewhere in the Mediterranean region (Lewin *et al.* 1995; Fuller *et al.* 1998). These conditions may have been enhanced by extreme seasonality during OIS 2 in which precipitation was concentrated during the winter months (Prentice *et al.* 1992).

While river activity took place along the valley axes, wind activity brought about sand transport and deposition across the remaining parts of the coastal plain. This is clearly seen at Calo d'es Cans where section A, which is nearest the channel, preserves the best record of river activity, and section C which is most distant from the channel does not include fluvial sediments, but is dominated by wind-blown sands. Section B, which is in an intermediate location, records both wind and river deposits. These wind blown sands are composed primarily of beach sands, often with a derived marine fauna, and represent the re-working of beach material deposited during the high sea-levels of OIS 5e and 5a, and sea-bed sand exposed by the fall of sea level during the colder episodes.

Aeolian sand deposition took place extensively during OIS 6, although the upper part of this unit has since been truncated by the shoreline erosion that took place during OIS 5e prior to beach deposition. Further deposition of wind-blown sand also occurred during OIS 5d and OIS 4, both periods being associated with the formation of discontinuous small dunes. Large, well defined dunes were formed during OIS 2, covering much of the coastal plain. In many respects the landscapes of OIS 6 and OIS 2 were very similar, consisting of a series of coarse grained alluvial fans at the valley mouths and extensive sand dune fields across the intervening lowland plain.

Loess deposition

Wind-blown silt or loess was also deposited during OIS 5c and OIS 4. The older deposit consists of a thin bed of silt that has since been modified by soil formation. The younger deposit is more extensive and forms a consistent bed across much of the area. The mineralogy of these units suggest that this material was derived from an extensive region rather than locally, but that the climate in which it formed was moist and suitable for vegetation growth and soil development with translocation of iron and carbonate minerals. The timing of this period of loess formation does not coincide with current understanding of the main periods of loess formation associated with anticyclonic weather systems and sediment supplies generated by the North European ice sheet, and may reflect seasonal dust flux or re-working of loessic material already deposited elsewhere.

Responses to changes of climate

Although the resolution of this study is not sufficient to identify the detailed processes that are involved in the changes of climate and environment, it is possible, from the detail that is available, to infer the main factors that have been responsible for these changes. Universally, a change from a temperate climate with extensive vegetation cover and soil development to a colder climate with less extensive vegetation cover has been accompanied by landscape instability in the form of river erosion and deposition, and aeolian sand transport and deposition. This has come about because of two independent factors. Firstly, the breakdown of vegetation cover, along with the occurrence of frost action in the soils and in jointed bedrock of the upper parts of the catchment, has resulted in surface runoff and a ready supply of erodible/transportable material. This, in turn, has resulted in the stripping-off of the

relatively deep soils formed in the preceding warmer periods, entrainment and transport by surface wash and mass movement of gelifracted bedrock, and river incision into the bed of the stream channels. The loss of capacity on the lower-angle slopes of the coastal plain, enhanced by the change in channel shape where the stream has exited the valley to flow across the fan, has resulted in fan deposition and burial of the lowland soils without significant erosion despite the absence of a protective vegetation cover.

The second factor is the fall of sea level which coincided with the deterioration of climate. The appearance of extensive sand plains across the shallow coastal region made available a ready supply of unlithified sand-size material that was transported across sparsely vegetated surfaces close to the coastal zone. The SEM and stable isotope studies of the carbonate cements indicate that the ready supply of mobile sand appears to have only limited duration because of the rapid process of lithification, both in the exposed coastal sediments and in the aeolian dunes. In this case it is likely that the process of aeolian sand deposition was a feature of the earlier phases of climatic deterioration, but much less important in the later stages and of minimal importance during the phases of climatic warming.

The evidence confirms the expectation that the magnitude of changes relate either to the scale of climate change or the duration of particular climatic conditions. For instance, there is no known geomorphological effect associated with the deterioration of climate recognized in the later part of OIS 5e, either because the change of climate was not sufficient to cause the geomorphic processes to cross critical thresholds of erosion and entrainment, or because the event was not long enough for sufficient quantities of material to be eroded and deposited. This point is also made by the scale of fluvial activity associated with each of the colder episodes, with by far the largest quantity of material deposited being associated with a period extending from the latter part of OIS 3 through the whole of OIS 2, a duration twice that of any of the other periods of climatic deterioration.

Conclusions

Stacked sequences of terrestrial sediments and soils, in sensitive geomorphological positions within the western Mediterranean provide detailed evidence of climatic and environmental changes through the period from the Last Interglacial to the Last Glacial Maximum.

Clearly defined geomorphological sites enable a reliable and comprehensive interpretation of the causes of landscape change because of the survival of soils and the incremental deposition of fluvial and aeolian sediments.

Both warm-temperate Mediterranean-type climates and moist cool-temperate climates experience relative landscape stability with effective soil development.

Climatic deterioration leads to a break-down of the established Mediterranean-type and cool temperate type vegetation cover, the desegregation of upland soils by ground-ice growth and melting, and the generation of transportable clasts from bedrock, by frost action. These conditions lead to extensive landscape instability caused by surface run-off in channels and on slopes, resulting eventually in river erosion on steeper slopes and fan deposition on the lowland margins.

Elsewhere, and particularly in the regions close to the present coastline, there is extensive aeolian sand transport, and deposition of material derived from newly exposed, unlithified sea-bed sediments.

There are some periods of extensive dust (loess) sedimentation which do not coincide with maximum glaciation elsewhere and are associated with relatively moist climate and a sparse vegetation cover.

This project was funded by NERC Research Grant Award GST/02/700'A. Thanks are expressed to E. Rhodes of the Luminescence Laboratory, Department of Geography, RHUL, G. Marriner and D. Mattey of the Stable Isotope Laboratory, Department of Geology, RHUL and G. Sykes of the Amino Acid Laboratory, Department of Earth Sciences, University of Cardiff. M. Seddan is also thanked for help with the identification of the marine mollusca. Referees B. Mauz and J. Woodward are thanked for there critical comments.

References

AITKEN, M.J. 1985. *Thermoluminescence Dating*. Academic Press, London.

BRITISH STANDARDS INSTITUTION 1985. *Methods for determination of particle size distribution*. BS812: Part 103: 1985. HMSO, London.

BUTZER, K.W. & CUERDA, J. 1962. Coastal stratigraphy of southern Mallorca and its implication of the Pleistocene chronology of the Mediterranean Sea. *Journal of Geology*, **70**, 398–416.

COAKLEY, J.P. & SYVITSKI, J.P.M. 1991. SediGraph Technique. *In*: SYVITSKI, J.P.M. (ed.) *Principles, Methods and Application of Particle Size Analysis*. Cambridge University Press, Cambridge.

CORNU, S., PATZOLD, J., BARD, E., MECO, J. & CUERDA-BARCELO, J. 1993. Palaeotemperature of the last interglacial period based on $\delta^{18}O$ of *Strombus bubonius* from the western Mediterranean Sea. *Palaeogeography, Palaeoclimatology, Palaeoecology*, **103**, 1–20.

CRAIG, H. 1965. The measurement of oxygen isotope palaeotemperature. *In*: TONGIORGI, E. (ed.) *Stable Isotopes in Oceanographic Studies and Palaeotemperature*. Consiglio Nazionale delle Richerche, Laboratorio di Geosiglia Nucleare, Pias, 161–182.

DE BEAULIEU, J.-L. & REILLE, M. 1992. The last climatic cycle at La Grande Pile (Vosges, France). A new pollen profile. *Quaternary Science Reviews*, **11**, 431–438.

EPSTEIN, S., BUCHSBAUM, R., LOWENSTAM, H. & UREY, H.C. 1953. Revised carbonate-water isotopic temperature scale. *Geological Society of America Bulletin*, **64**, 1315–1326.

FIELD, M.H., HUNTLEY, B. & MULLER, H. 1994. Eemian climate fluctuations observed in a European pollen record. *Nature*, **371**, 779–783.

FULLER, I.C., MACKLIN, M.G., LEWIN, J., PASSMORE, D.G. & WINTLE, A.G. 1998. River response to high-frequency climate oscillations in southern Europe over the past 200 k.y. *Geology*, in press.

GALE, S.J. & HOARE, P.G. 1991. *Quaternary Sediments: petrographic methods for the study of unlithified rocks*. Wiley, Chichester.

GUIOT, J., PONS, A., BEAULIEU, J.L. & REILLE, M. 1989. A 140,000-year continental climate reconstruction from two European pollen records. *Nature*, **338**, 309–313.

GRIP MEMBERS 1993. Climate instability during the last interglacial period recorded in the GRIP ice core. *Nature*, **364**, 203–207.

HAYS, P.D. & GROSSMAN, E.L. 1991. Oxygen isotopes in meteoric calcite cements as indicators of continental palaeoclimate. *Geology*, **19**, 441–444.

HEARTY, P.J. 1987. New data on the Pleistocene of Mallorca. *Quaternary Science Reviews*, **6**, 245–257.

——, MILLER, G., STEARNS, C. & SZABO, B. 1986. Aminostratigraphy of Quaternary shorelines in the Mediterranean basin. *Geological Society of America Bulletin*, **97**, 850–858.

HILLAIRE-MARCEL, C., GARIÉPY, C., GHALEB, B., GOY, J.-L., ZAZO, C. & BARCELO, J.C. 1996. U-Series measurements in Tyrrhenian deposits from Mallorca—further evidence for two Last Interglacial high sea-levels in the Balearic Islands. *Quaternary Science Reviews*, **15**, 53–62.

LECOLLE, P. 1985. The oxygen isotope composition of landsnail shells as a climatic indicator: applications to hydrogeology and palaeoclimatology. *Chemical Geology (Isotope Geoscience Section)*, **58**, 157–181.

LEWIN, J., MACKLIN, M.G. & WOODWARD, J.C. (eds) 1995. *Mediterranean Quaternary River Environments*. Balkema, Rotterdam.

MACKLIN, M.G., LEWIN, J. & WOODWARD, J.C. 1995. Quaternary Fluvial systems in the Mediterranean basin. *In*: LEWIN, J., MACKLIN, M.G. & WOODWARD, J.C. (eds) *Mediterranean Quaternary River Environments*. Balkema, Rotterdam, 1–25.

MAHER, B.A. & THOMPSON, R. 1992. Palaeoclimatic significance of the mineral magnetic record of the Chinese loess and palaeosols. *Quaternary Research*, **37**, 155–170.

—— & —— 1995. Palaeorainfall reconstruction from pedogenetic magnetic susceptibility variations in Chinese loess and palaeosol. *Quaternary Research*, **44**, 383–391.

MARSHALL, J.D. 1992. Climatic and oceanographic isotopic signals from the carbonate rock record and their preservation. *Geological Magazine*, **129**, 143–160.

MASLIN, M. & TZEDAKIS, C. 1996. Sultry Last Interglacial gets sudden chill. *EOS*, **77**, 353–354.

MENG, X.M., DERBYSHIRE, E. & KEMP, R.A. 1997. Origin of the magnetic susceptibility signal in Chinese loess. *Quaternary Science Reviews*, **16**, 833–839.

O'NEIL, J.R., CLAYTON, R.N. & MAYEDA, T.K. 1969. Oxygen isotope fractionation in divalent metal carbonates. *The Journal of Chemical Physics*, **51**, 5547–5558.

PERRY, A. 1981. Mediterranean climate—a synoptic reappraisal. *Progress in Physical Geography*, **5**, 107–113.

PONS, A. & REILLE, M. 1988. The Holocene and Upper Pleistocene pollen record from Padul (Granada, Spain): a new study. *Palaeogeography, Palaeoclimatology and Palaeoecology*, **66**, 243–263.

PRENTICE, I.C., GUIOT, J. & HARRISON, S.P. 1992. Mediterranean vegetation, lake levels and palaeoclimate at the last glacial maximum. *Nature*, **360**, 658–660.

QUADE, J., CERLING, T.E. & BOWMAN, J.R. 1989. Systematic variation in the carbon and oxygen isotopic composition of Holocene soil carbonate along elevation transects in the southern Great Basin, USA. *Geological Society of America Bulletin*, **101**, 464–475.

——, SOLOUNIAS, N. & CERLING, T.E. 1994. Stable isotopic evidence from palaeosol carbonates and fossil teeth in Greece for forest or woodlands over the past 11 Ma. *Palaeogeography, Palaeoclimatology, Palaeoecology*, **108**, 41–53.

REILLE, M. & DE BEAULIEU, J.-L. 1990. Pollen analysis of a long upper Pleistocene continental sequence in a Velay maar (Massif Central France). *Palaeogeography, Palaeoclimatology, Palaeoecology*, **80**, 35–48.

RHODES, E.J. 1988. Methodological considerations in the optical dating of Quartz. *Quaternary Science Reviews*, **7**, 395–400.

ROGNON, P. 1987. Aridification and abrupt climatic events on the Saharan northern and southern margins, 20,000 years BP to present. *In*: BERGER, W.H. & LABEYRIE, C.D. (eds) *Abrupt Climatic Change: Evidence and Implications*. Reidel, Dordrecht, 209–220.

ROSE, J. & MENG, X. 1998. River activity in small catchments over the last 140 ka, northeast Mallorca, Spain. *In*: BROWN, A.G. & QUINE, T. (eds) *Fluvial processes and environmental change*. Wiley, Chichester, In Press.

SHACKLETON, N.J. 1987. Oxygen isotopes, ice volume and sea level. *Quaternary Science Reviews*, **6**, 183–190.

SYKES, G. 1991. Amino acid dating. *In*: SMART, P.L. & FRANCES, P.D. (eds) *Quaternary Dating Methods—a User's Guide*. Quaternary Research Association Technical Guide **4**, 161–176.

TUCKER, M. & WRIGHT, V.P. 1990. *Carbonate Sedimentology*. Blackwell, Oxford.

TZEDAKIS, P.C. & BENNETT, K.D. 1995. Interglacial vegetation succession: a view from southern Europe. *Quaternary Science Reviews*, **14**, 967–982.

WATTS, W.A., ALLEN, J.R.M. & HUNTLEY, B. 1996. Vegetation history and palaeoclimate of the Last Glacial period at Lago Grande di Monticchio, southern Italy. *Quaternary Science Reviews*, **15**, 133–153.

WEST, R.G. 1980. Pleistocene forest history in East Anglia. *New Phytologist*, **85**, 571–622.

WOOD, P.L. 1997. *Dating and origin of Late Quaternary catastrophic shoreline activity around the Mediteranean Sea*. PhD thesis, University of London.

YAALON, D.H. 1997. Soil in the Mediterranean region: what makes them different? *Catena*, **28**, 157–169.

ZAZO, C., BARDAJÍ, T., DABRIO, C.J., GOY, J.L. & HILLAIRE MARCEL, C. 1998. Record of Late Pliocene and Quaternary sea-level changes in coastal settings, Southeast Spain - Excursion A7. *In*: *15th International Congress of Sedimentology Field Guide*. IAS, Alicante, 151–169.

Received 21 March 1998; revised typescript accepted 20 June 1998.
Scientific editing by Ian Fairchild.